X-ray resonant scattering study of spin-density waves in a superlattice

1999 J. Phys.: Condens. Matter 11 L139

(http://iopscience.iop.org/0953-8984/11/15/002)

J. Phys.: Condens. Matter **11** (1999) L139–L146. Printed in the UK PII: S0953-8984(99)01953-0

LETTER TO THE EDITOR

X-ray resonant scattering study of spin-density waves in a superlattice

J P Goff†, R S Sarthour†, D F McMorrow‡, F Yakhou§, A Stunault§, A Vigliante‖, R C C Ward† and M R Wells†

† Department of Physics, Clarendon Laboratory, Oxford University, Parks Road, Oxford OX1 3PU, UK

‡ Condensed Matter Physics and Chemistry Department, Risø National Laboratory, DK-4000 Roskilde, Denmark

§ European Synchrotron Radiation Facility, BP 220, F-38043, Grenoble Cedex, France

‖ Department of Physics, Brookhaven National Laboratory, Upton, NY 11973, USA

Received 19 February 1999

Abstract. The magnetic structures of Nd/Pr superlattices have been investigated using x-ray magnetic resonant scattering. Magnetic dipole resonances were observed at the L_{II} ($2p_{1/2} \rightarrow 5d$) edges of both components of the superlattices, proving that a coherent spin-density wave is established in the 5d bands of both elements. Multi-$\boldsymbol{q}$ magnetic structures were induced in the Pr, and the two components of the superlattice were found to adopt identical magnetic modulation vectors. Magnetic superlattice peaks were observed in $\boldsymbol{Q}$-scans at both edges and from these we were able to determine the magnetization profiles in each component of the superlattice separately. From the width of the magnetic peaks in the wave-vector, ΔQ, we were able to measure the magnetic coherence of the Nd, and the results demonstrate that the observed spin-density wave in the Pr is responsible for the coupling between successive Nd blocks.

The development of molecular beam epitaxy has enabled the controlled growth of single-crystal layered structures with almost atomic-plane precision. As a consequence it is possible to introduce an artificial periodicity and create superlattice structures, potentially with tailor-made physical properties.

The discovery of the propagation of magnetic ordering through nonmagnetic spacer layers in rare-earth superlattices has opened a new window on the nature of exchange coupling in the metallic state [1]. It is generally accepted that long-range order is established by the magnetic material inducing a spin-density wave in the conduction band of the nonmagnetic element (the (5d, 6s) electrons in the case of the rare earths), which then propagates the order to the next magnetic block. In the case of transition-metal superlattices, direct evidence for the existence of induced ordering has been obtained using x-ray magnetic circular dichroism (XMCD) [2, 3]. This technique measures the spin and orbital moments in each component averaged over the superlattice structure, but cannot determine directly the spatial modulation of the magnetization. A diffraction method, such as x-ray magnetic resonant scattering (XMRS), shares the species sensitivity of XMCD, and has the added advantage that spatial information is retained [4–6]. Antiferromagnetic ordering within individual blocks of a superlattice may therefore be studied using this technique. Furthermore, by measuring the magnetic diffraction harmonics from the superlattice structure at the resonant edge of each component, it is possible, in principle, to determine the magnetization profile of each element independently. In this letter

0953-8984/99/150139+08$19.50

we report results from Nd/Pr superlattices, where we have been able to study the magnetic ordering of the two components of a superlattice separately for the first time using magnetic x-ray diffraction.

Nd and Pr sit adjacent to each other in the light rare earth series. In the bulk state both elements adopt the dhcp crystal structure, but have very different magnetic properties. The localized 4f moments on the hexagonal sites in Nd order below $T_N \sim 19.9$ K, with an antiferromagnetic coupling between hexagonal layers and an incommensurate sinusoidal modulation in the basal plane [7]. As the temperature is lowered, a series of multi-$\boldsymbol{q}$ magnetic structures are observed [8, 9]. Pr has a nonmagnetic singlet as its ground state and does not exhibit long-range magnetic ordering until it is induced by the hyperfine interaction at $T_N \sim 50$ mK [10, 11]. It has been found that magnetic order may be induced at higher temperatures by perturbations such as the application of uniaxial pressure or an external magnetic field [12, 13], or by alloying with Nd, and in this way Pr constitutes an almost critical system.

Neutron diffraction studies of Nd/Pr superlattices have revealed a number of new phenomena [14], but since in this case the magnetic scattering is dominated by the contribution from the 4f moments, any information on the spin-density wave in the (5d, 6s) bands is to some extent model dependent. The Nd magnetic order on the hexagonal sites propagates coherently through the Pr, while the cubic site order is confined to single Nd blocks. For thinner blocks of Pr ($\sim$ 20 atomic planes) the Nd induces long-range order of the Pr 4f moments at all temperatures below T_N, so that a uniform magnetic structure is formed throughout the superlattice. For thicker Pr blocks ($\sim$ 33 atomic planes) the Pr retains its singlet ground state close to T_N, and it is only on cooling that a 4f moment is induced in the Pr. One of the attractive features of Nd/Pr for studies using synchrotron x-rays is that the in-plane incommensurate component to the magnetic modulation moves the magnetic scattering away from [00l] to a region where the structural background is low. It also illustrates how XMRS can provide new information on the magnetic interactions in artificial metallic superlattices. By isolating the magnetic scattering from the Pr we obtain direct information on the nature of the induced magnetic ordering. The energy and polarization dependence of the scattering at the resonances probes the electronic states of the magnetic species. Furthermore, the narrow wave-vector transfer resolution achieved using x-rays enables the multi-$\boldsymbol{q}$ magnetic structures to be studied more closely than before. This latter feature also allows a more accurate determination of the magnetic coherence through the superlattice, and this provides greater understanding of the mechanism of interlayer coupling.

XMRS at the L edges of the rare earth metals is dominated by virtual electric dipole (E1) transitions from a 2p core level to the 5d bands [5]. Magnetic x-ray diffraction therefore gives direct information on the conduction-electron spin-density wave responsible for the propagation of magnetic order in rare-earth metals and superlattices. In this sense it gives complementary information to neutron diffraction, which tends to be dominated by scattering from the ordered 4f moments. The resonant cross section may be written down in a convenient form appropriate to Nd/Pr if we assume that the magnetic moments are sinusoidally modulated with a wave-vector $\boldsymbol{q}$, and that we use polarization analysis to measure the rotated component of the scattering (here labelled π–σ and explained below) [15]. For scattering vectors close to [00l] the resonant cross section may then be written

$$\left(\frac{\mathrm{d}\sigma}{\mathrm{d}\Omega}\right)_{E1}^{\pi-\sigma} \approx \frac{M^2 P^2 \cos^2\theta}{(\hbar\omega_0 - \hbar\omega)^2 + (\Gamma/2)^2}\delta(\boldsymbol{Q} - \boldsymbol{G} \pm \boldsymbol{q}) \tag{1}$$

where M is proportional to the square of the radial matrix element connecting the 2p and 5d states, $\hbar\omega_0$ is the energy of the appropriate L resonance of half width Γ, θ is the Bragg

angle, and $\boldsymbol{G}$ is a reciprocal lattice vector. The sensitivity to the magnetism comes from the polarization factor

$$P = n_e(\uparrow) - \frac{n_h \Delta/2}{\hbar\omega_0 - \hbar\omega - \mathrm{i}\Gamma/2} - n_h\delta \tag{2}$$

where $n_e(\uparrow)$ is the net number of spin-up electrons in the 5d band, n_h the number of holes, Δ the exchange splitting and δ depends on the difference in radial matrix elements for spin-up and spin-down electrons [5]. The sensitivity of XMRS to the 5d polarization was exploited by Everitt *et al* [16] to measure the polarization of the 5d bands at the Lu sites in a Dy–Lu alloy. The resonant enhancement at the L_{II} edge over the nonresonant signal is found to be 300 for Nd metal [17] and very large for Pr in Ho:Pr alloys [18]. These elements are therefore ideally suited to XMRS, and here we demonstrate the potential for determining the magnetization profiles in a superlattice structure.

Single-crystal *c*-axis Nd/Pr superlattices were grown using molecular beam epitaxy with compositions $[Nd_{20}Pr_{20}]_{80}$ and $[Nd_{33}Pr_{33}]_{50}$, where the subscripts labelling the elements refer to the number of atomic planes in the average bilayer and the last subscript to the number of bilayers. The x-ray scattering experiments were performed mainly using the four-circle diffractometer at ID20 of the European Synchrotron Radiation Facility, with additional studies carried out using X22C at Brookhaven National Laboratory. The samples were mounted with (h0l) in the scattering plane of the diffractometer. At ID20 the polarization of the scattered beam was analysed by a sapphire crystal mounted on the 2θ arm of the diffractometer. For the horizontal scattering geometry employed on ID20 the incident photon beam is predominantly linearly polarized ($\geqslant 98\%$) in this plane, which by convention is labelled π (the perpendicular component being σ). By rotating the polarization analyser around the scattered beam it was possible to measure either the π–σ or π–π components of the scattering.

In order to characterize the chemical structure, scans of the wave-vector transfer $\boldsymbol{Q}$ were performed along the [00l] direction through the (π–π) charge scattering at (004), and superlattice peaks were observed displaced from the average Bragg reflection by $2\pi n/L$, where L is the bilayer repeat distance and n is an integer. The data were fitted to the structural model of Jehan *et al* [19] in which the number of planes and the interplanar spacing of each layer are allowed to vary, and a tanh function is used to represent the variation of concentration and d-spacing at the interfaces. This analysis showed that the structures of the superlattices were close to their target specifications and that interdiffusion at the interfaces was restricted to 4 atomic planes at most.

A search for (π–σ) magnetic scattering was made at the Nd and Pr L_{II} edges by performing scans of $\boldsymbol{Q}$ along the (h03) direction at $T \sim 3$ K. Two magnetic reflections are detected at $\boldsymbol{Q} \sim (0.106,\ 0,\ 3)$ and $(0.12, 0, 3)$ close to the ordering wave-vectors of bulk Nd. The peaks are observed at identical positions at the two edges, indicating that the superlattices exhibit uniform magnetic structures. By analogy with bulk Nd, the two components of the scattering are from different domains of the quadruple-$\boldsymbol{q}$ structure [9], and the measurements at the Pr edge are the first direct observation of a multi-$\boldsymbol{q}$ magnetic structure in Pr.

Figure 1 presents the scattering measured from $[Nd_{33}Pr_{33}]_{50}$ in scans of the x-ray energy for fixed $\boldsymbol{Q} = (0.106,\ 0,\ 3)$ at $T \sim 3$ K. The scattering was observed to resonate at 6.440 keV and 6.722 keV, close to the energies of the dipole transitions at the L_{II} edges of Pr and Nd respectively. As this transition is from a $2p_{1/2}$ core state to the 5d bands, we can immediately conclude from the existence of the resonances at the two edges that the 5d bands are magnetically polarized in both elements. We note that shoulders are evident in the energy scans at the two edges, indicating that there are at least two resonances in each case. Further studies are required to understand the origin of this lineshape.

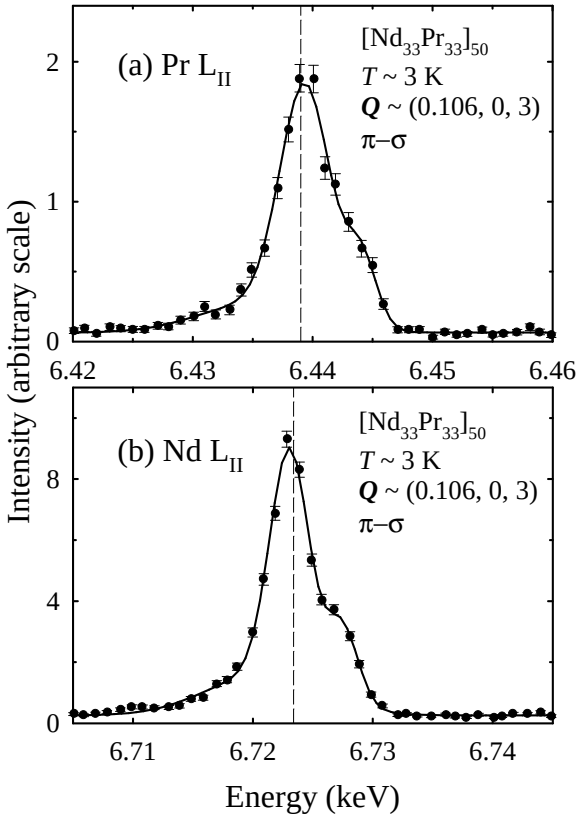

Figure 1. Energy scans at 3 K with $\boldsymbol{Q}$ fixed at (0.106, 0, 3), showing the resonant enhancement at (a) the Pr L_{II} and (b) the Nd L_{II} edges. Solid lines are guides to the eye and dashed lines indicate the positions of the absorption edges.

The temperature dependence of the scattering is summarized in figure 2 which compares scans of $\boldsymbol{Q}$ in the $\boldsymbol{c}^*$ direction through the magnetic peaks at the Pr and Nd L_{II} edges at selected temperatures for $[Nd_{33}Pr_{33}]_{50}$. These scans give information on the propagation of the magnetic order through the superlattice. Magnetic superlattice peaks are detected displaced by $2\pi/L$ from the magnetic Bragg peak. The moment profile through the magnetic blocks determines the intensity of the superlattice peaks, and the presence of strong superlattice peaks either side of the main magnetic Bragg reflection indicates a near-square-wave moment profile. This is observed at all temperatures for Nd, and at $T \sim 3$ K for Pr. At higher temperatures the superlattice peaks decrease in intensity relative to the main magnetic Bragg peak at the Pr edge, and can no longer be detected by $T \sim 10$ K. The broadening of the peaks at the higher temperatures shows a decrease in the coherence of the magnetism.

To model the data, at the Nd edge the magnetic form factors are taken to be unity at the Nd sites, and zero at the Pr sites, and vice-versa at the Pr resonance. The moment directions alternate for successive hexagonal planes and, since the structural parameters are determined from the charge scattering, the integrated intensities of the peaks in figure 2 are determined solely by the polarization profiles. The magnetic scattering has been calculated using the polarization profiles in figure 3, and this is shown as the solid lines in figure 2. The widths are fixed at the experimentally determined values. The polarization follows the concentration

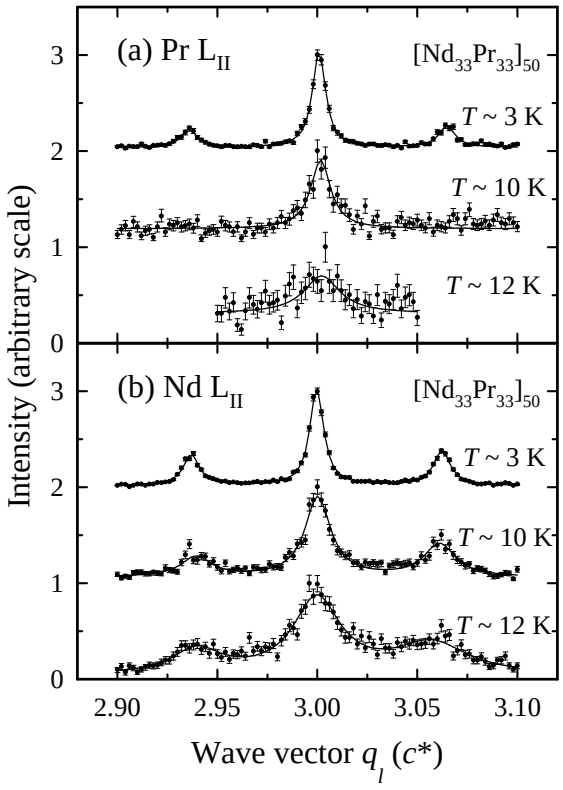

Figure 2. The temperature dependence of the scans of $\boldsymbol{Q}$ in the $\boldsymbol{c}^*$ direction through the π–σ magnetic Bragg reflection at $(q_h, q_k, 3)$ (a) at the Pr L_{II} and (b) at the Nd L_{II} edges.

profile at all temperatures at the Nd resonance (figure 3). The profile in the Pr blocks has been modelled as an exponential fall-off of the induced moment away from the interface with Nd. The results for Pr at $T \sim 3$ K show that an almost uniform moment is induced across the 100 Å-thick Pr block at low temperatures. However, by $T \sim 10$ K the induced polarization at the centre of the thick Pr blocks is very small, see figure 3.

The integrated intensities of the magnetic scattering, at the Pr and Nd edges have been measured as a function of temperature for both samples. The magnitude of the average polarization of the 5d band of Pr relative to that of Nd, P_{Pr}/P_{Nd}, may then be obtained using [16]

$$\frac{P_{Pr}}{P_{Nd}} = \frac{\langle r\rangle_{Nd}^2}{\langle r\rangle_{Pr}^2}\sqrt{\frac{C_{Nd}I_{Pr}}{C_{Pr}I_{Nd}}} \tag{3}$$

where $\langle r\rangle$ corresponds to the species-specific radial matrix element, C the concentration of each element in the superlattice, and I is the integrated intensity of the magnetic peak normalized by the charge scattering at each energy. The radial matrix elements have been calculated for Nd and Ce [20], and we interpolate between these to obtain the value for Pr. For the L_{II} edge, $\langle 2p_{1/2}|r|5d\rangle = 0.00574$ for Nd and 0.00597 for Pr. By dividing the magnetic intensity by the charge scattering peaks at each energy, we correct for absorption and the dependence of the incident x-ray intensity on energy approximately. Figure 4(a) shows that P_{Pr}/P_{Nd} remains approximately constant at 0.43 for $[Nd_{20}Pr_{20}]_{80}$ at all temperatures studied. The fact that the

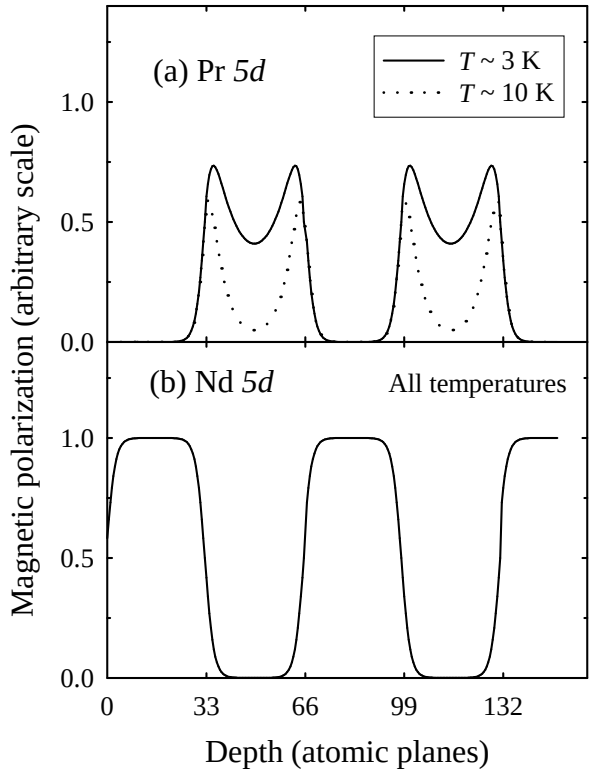

Figure 3. The amplitude of the magnetic polarization of the 5d bands (a) for Pr and (b) for Nd, as a function of depth, used to calculate the scattering in figure 2.

polarization of the Pr 5d band is comparable to Nd provides evidence that localized ordering of the Pr 4f moments is also induced. For $[Nd_{33}Pr_{33}]_{50}$, the average polarization in the Pr decreases rapidly at higher temperatures, and this is consistent with the derived fall-off of the induced order away from the Nd interface, as shown in figure 3.

The magnetic correlation lengths, ξ, shown in figure 4(b), were obtained from the widths of the $\boldsymbol{c}^*$ scans through the magnetic reflections at the Nd L_{II} edge using the relation $\xi \sim 2\pi/\Delta Q$. For $[Nd_{20}Pr_{20}]_{80}$ the magnetic order is coherent over many bilayer repeats at all temperatures, and ξ is comparable to the structural correlation length. However, there is a dramatic decrease in ξ for $[Nd_{33}Pr_{33}]_{50}$ above $T \sim 8$ K, indicating a decoupling of the Nd blocks. This is correlated with the reduction of the induced polarization in the centre of the Pr blocks, and this directly confirms that the Pr conduction-electron spin-density wave is responsible for the propagation of the Nd magnetic order. The results for $[Nd_{33}Pr_{33}]_{50}$ do not agree with those obtained using neutrons for a sample with the same nominal composition [14], possibly due to resolution effects. We note that the correction due to instrumental resolution is negligible for these x-ray measurements. This technique greatly extends the accessible range of correlation lengths, and allows a simpler understanding of the magnetic coupling in Nd/Pr superlattices to emerge.

In summary, magnetic resonances were observed for both the Nd and Pr L_{II} edges, showing that the 5d bands are magnetically polarized in both elements. The two components of the superlattice are found to adopt identical multi-$\boldsymbol{q}$ magnetic structures. The amplitude of the induced conduction-electron spin-density wave has been determined as a function of depth in

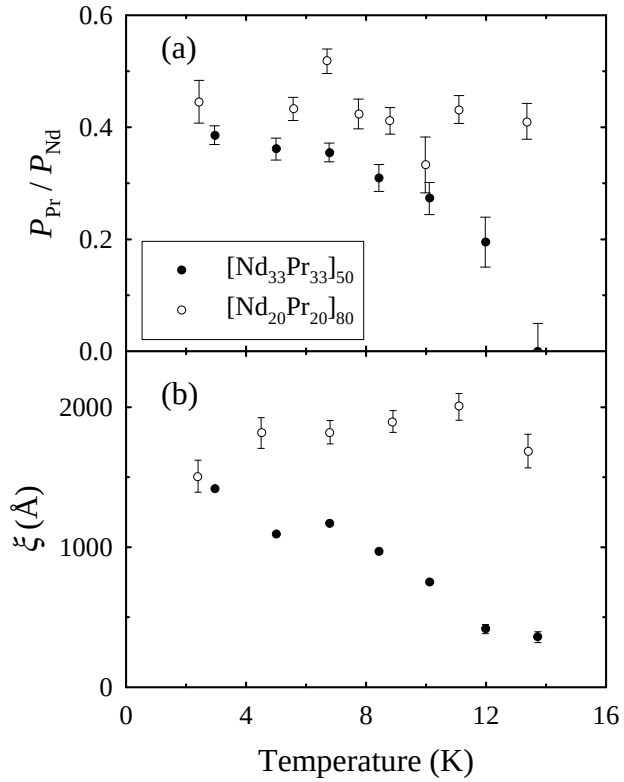

Figure 4. (a) The polarization of the Pr 5d band relative to Nd, and (b) the magnetic correlation length, ξ, as a function of temperature.

the Pr blocks, and the coherence of the magnetism has been measured. The results provide new understanding of the induced magnetic ordering and the interlayer coupling mechanism in Nd/Pr superlattices.

We would like to thank D Gibbs, J P Hill, D Wermeille and E Lidstrom for help and advice. Financial assistance from the EPSRC in the UK, CAPES in Brazil, and the EU is gratefully acknowledged, and work at Brookhaven is supported under Grant No DEAC0298CH10886.

References

[1] Salamon M B, Sinha S, Rhyne J J, Cunningham J E, Erwin R W, Borchers J A and Flynn C P 1986 *Phys. Rev. Lett.* **56** 259
[2] Schutz G, Stahler S, Knulle M and Fischer P 1993 *J. Appl. Phys.* **73** 6430
[3] Samant M G, Stohr J, Parkin S S P, Held G A, Hermsmeier B D, Herman F, van Schilfgaarde M, Duda L-C, Mancini D C, Wassdahl N and Nakajima R 1994 *Phys. Rev. Lett.* **72** 1112
[4] Gibbs D, Harshman D R, Isaacs E D, McWhan D B, Mills D, and Vettier C 1988 *Phys. Rev. Lett.* **61** 1241
[5] Hannon J P, Trammel G T, Blume M and Gibbs D 1988 *Phys. Rev. Lett.* **61** 1245
[6] Gibbs D, Grubel G, Harshman D R, Isaacs E D, McWhan D B, Mills D and Vettier C 1991 *Phys. Rev.* B **43** 5663
[7] Moon R M, Cable J W and Koehler W C 1964 *J. Appl. Phys.* **35** 1041
[8] McEwen K A, Forgan E M, Stanley H B, Bouillot J and Fort D 1985 *Physica* B **130** 360
[9] Forgan E M, Gibbons E P, McEwen K A and Fort D 1989 *Phys. Rev. Lett.* **62** 470
[10] McEwen K A and Stirling W G 1981 *J. Phys. C: Solid State Phys.* **14** 157

[11] Møller H B, Jensen J Z, Wulff M, Mackintosh A R, McMasters O D and Gschneider K A 1982 *Phys. Rev. Lett.* **49** 482
[12] McEwen K A, Stirling W G and Vettier C 1978 *Phys. Rev. Lett.* **41** 343
[13] McEwen K A, Cock G J, Roeland L W and Mackintosh A R 1973 *Phys. Rev. Lett.* **30** 287
[14] Goff J P, Bryn-Jacobsen C, McMorrow D F, Ward R C C and Wells M R 1997 *Phys. Rev.* B **55** 12 537
[15] Hill J P and McMorrow D F 1996 *Acta Crystallogr.* A **52** 236
[16] Everitt B A, Salamon M B, Park B J, Flynn C P, Thurston T and Gibbs D 1995 *Phys. Rev. Lett.* **75** 3182
[17] Watson D, Nuttall W J, Forgan E M, Perry S C and Fort D 1998 *Phys. Rev.* B **57** 8095
[18] Vigliante A, Christensen M J, Hill J P, Helgesen G, Sørensen S Aa and McMorrow D F 1998 *Phys. Rev.* B **57** 5941
[19] Jehan D A, McMorrow D F, Cowley R A, Ward R C C, Wells M R, Hagmann N and Clausen K N 1993 *Phys. Rev.* B **48** 5594
[20] Hamrick M 1994 *PhD thesis* Rice University